

Oscillation-Test Methodology for Low-Cost Testing of Active Analog Filters

Karim Arabi, *Member, IEEE*, and Bozena Kaminska, *Senior Member, IEEE*

Abstract—The oscillation-test strategy is a low cost and robust test method for mixed-signal integrated circuits. Being a vectorless test method, it allows one to eliminate the analog test vector generator. Furthermore, as the oscillation frequency is considered to be digital, it can be precisely analyzed using pure digital circuitry and can be easily interfaced to test techniques dedicated to the digital part of the circuit under test (CUT). This paper describes the design for testability (DFT) of active analog filters based on oscillation-test methodology. Active filters are transformed to oscillators using very simple techniques. The tolerance band of the oscillation frequency is determined by a Monte Carlo analysis taking into account the nominal tolerance of all circuit under test components. Discrete practical realizations and extensive simulations based on CMOS 1.2 μm technology parameters affirm that the test technique presented for active analog filters ensures high fault coverage and requires a negligible area overhead. Finally, the DFT techniques investigated are very suitable for automatic testable filter synthesis and can be easily integrated in the tools dedicated to automatic filter design.

Index Terms—Active filter, analog testing, built-in self-test (BIST), design for testability (DFT), integrated circuits, oscillation-test.

I. INTRODUCTION

THE design for testability (DFT) of analog and mixed-signal circuits has received considerable attention of industry in order to decrease the production cost of mixed-signal application-specific integrated circuits (ASIC's). The specifications of analog circuits are usually very broad, which results in long testing times, poor fault coverage and the necessity for dedicated test equipment. DFT of analog circuits is a challenging task due to the dependency of circuit parameters on component variations and the variety of analog building blocks. The control, test stimulus generator and measurement circuitry may be placed on the same chip to present test pass or fail result which is known as built-in self-test (BIST) approach [1]–[3]. Existing analog DFT techniques may be divided into two main categories. The first category deals with increasing the controllability and observability of the internal nodes without proportionally increasing the number of test pins [4]–[10]. The other is to alter the circuit under test (CUT) function and generate a signal which reflects the CUT performance [11]–[14]. The circuit transformation aims to ease the test problem by generating a signal which can

be simply processed to determine the CUT malfunction. In this context, a new test method, called oscillation-test strategy, based on transformation of the CUT to an oscillator [11]–[13] has been recently introduced. In this paper, we present a practical and low-cost test approach for active analog filters based on oscillation-test methodology.

The paper is organized as follows. Section II is devoted to presenting the oscillation-test method. Techniques to transform a filter under test to an oscillator are briefly presented in Section III. Section IV introduces our analog fault modeling. In Section V, the results obtained from some case studies are presented. Some practical considerations and discussions are finally presented in Section VI.

II. OSCILLATION-TEST STRATEGY DESCRIPTION

This test method is based on partitioning a complex analog circuit into functional building blocks, such as amplifier, operational amplifier (OA), comparator, Schmitt trigger, filter, voltage reference, oscillator, phase locked-loop (PLL), etc., or a combination of these blocks. During test mode, each building block is converted to a circuit which oscillates. The oscillation frequency f_{osc} of each building block can be expressed as a function of either its components or its important parameters. The building blocks which inherently generate a frequency, such as oscillators, do not need to be rearranged, and their output frequency is directly evaluated. The test is performed by evaluating the oscillation frequency.

The observability of a faulty component (or parameter) is defined as the sensitivity of the oscillation frequency f_{osc} with respect to the variations of the component (or the parameter). A fault is said to be detectable if it causes a reasonable deviation of the oscillation frequency from its tolerance band. The tolerance band of f_{osc} for each CUT is determined based on a Monte Carlo analysis of the converted CUT taking into account the nominal tolerance of all important technology and design parameters. To increase the observability of a defect in a component (or a fault in a parameter), the sensitivity of the oscillation frequency with respect to that component (or parameter) should be increased. In other words, during the process of converting the CUT to an oscillator, the oscillator architecture must be chosen so as to ensure the maximum possible CUT component contribution in determining the oscillation frequency. If necessary, more than one oscillator may be derived from a CUT to increase fault coverage. Existing faults in the CUT related to components (or parameters) which are involved in the oscillator structure manifest themselves as a deviation of the oscillation frequency. Therefore, the deviation

Manuscript received August 8, 1996.

K. Arabi is with the Department of Electrical Engineering, École de Technologie Supérieure (ÉTS), Montreal, P.Q., Canada H3C 1K3 (e-mail: bozena@vlsi.polymtl.ca).

B. Kaminska is with Opmaxx, Inc., Beaverton, OR 97005 USA.

Publisher Item Identifier S 0018-9456(99)06684-X.

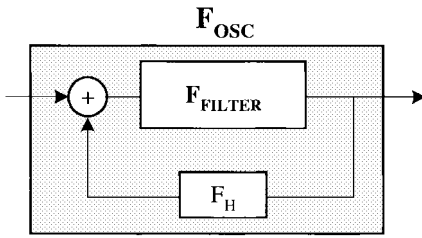


Fig. 1. General approach to converting the circuit under test to an oscillator (F_{FILTER} : transfer function of the filter under test, F_{OSC} : transfer function of an oscillator, and F_H : transfer function of feedback loop).

of the oscillation frequency from its nominal value may be employed to confirm a fault.

The equivalent rms noise of the CUT is normally much smaller than the amplitude of the oscillation signal and therefore cannot affect its frequency. If the equivalent rms noise is considerable, it may only cause a small jitter in the oscillation signal. In practice, many oscillation cycles are used to estimate the oscillation frequency, and consequently the jitter is averaged and, due to the random nature of noise, is canceled. However, if the oscillation signal amplitude is as small as the CUT equivalent rms noise, which is far from the case in practice, the oscillation frequency will be seriously affected by the noise.

III. FILTER-TO-OSCILLATOR CONVERSION TECHNIQUES

A brief survey of techniques we have found to be efficient in converting an active filter to an oscillator is presented in this section. For each type of active filter, various techniques can be easily found to transform it to an oscillator. Naturally, each second- or higher-order system has the potential for oscillation. This ability can be used to convert the filter under test to an oscillator by establishing the oscillation condition (Barkhausen criterion [15]) in its transfer function. For example, second-order active filters can be converted to oscillators by making their quality factor (Q_F) very high during test mode, which is equivalent to shifting its poles on the imaginary axis.

A more general technique is to add a feedback loop to the filter under test and then adjust the feedback element to produce sustained oscillations. The feedback loop may be positive, negative, or a combination of both. To simplify the mathematical presentation, in the following we consider the conversion of a filter under test using a positive feedback loop, as shown in Fig. 1. However, the feedback element may incorporate the effect of negative or mixed feedbacks. For example, a positive feedback loop with a feedback element having a negative sign results in a negative feedback. The transfer function of the new system F_{OSC} with a positive feedback is given by

$$F_{\text{OSC}} = \frac{F_{\text{FILTER}}}{1 - F_{\text{FILTER}}F_H} \quad (1)$$

where F_{FILTER} represents the original transfer function of the filter and F_H is the transfer function of the feedback element. The oscillation frequency ω_{OSC} and the oscillation condition are obtained from

$$F_{\text{FILTER}}(j\omega)F_H(j\omega) = 1 \quad (2)$$

or equivalently

$$\text{Re}(F_{\text{FILTER}}(j\omega)F_H(j\omega)) = 1 \quad (3)$$

$$\text{Im}(F_{\text{FILTER}}(j\omega)F_H(j\omega)) = 0. \quad (4)$$

This condition is known as the Barkhausen criterion. The Barkhausen criterion states that at the frequency of oscillation ω_{OSC} the signal must traverse the loop with no attenuation and no phase shift. For positive feedback, the phase shift must be zero, but for negative feedback, the phase shift must be 180° , to cancel the feedback sign and produce a total phase shift of zero.

As an example to clarify the Barkhausen criterion, we consider the case of a band-pass system which is composed of a first-order low-pass and high-pass system cascaded together. The output of the system is directly connected to its input to establish positive feedback. The low-pass system has a pole at its cutoff frequency and therefore its phase goes from zero to -90° as ω goes from zero to infinity. The high-pass system has a zero at the origin and a pole at its cutoff frequency; hence its phase goes from $+90^\circ$ to zero as ω goes from zero to infinity. At a specified frequency, the phase lead and lag effects cancel each other out and the overall phase shift will be zero. If the loop gain at that frequency is slightly greater than unity, the system produces sustained oscillations at that frequency. In fact, in a band-pass system with its output connected to the input, existing noise is band-pass filtered and amplified in the loop. The frequency components which pass through the band-pass system are reapplied to the system by means of the positive feedback and the same procedure is repeated, resulting in an oscillating signal constituted from the frequency components which pass through the band-pass system. The amplitude of the oscillations is limited by the nonlinear effects of the system. The oscillation frequency is determined by the bandwidth and the gain of the system. It should be noted that the presence of harmonic terms in the oscillation frequency due to the limited Q_F and nonlinear characteristics of the band-pass system causes a phase shift $\Delta\varphi$. To compensate for this phase shift, the oscillation frequency is shifted by an amount of $\Delta\omega$ to supply a phase shift of $-\Delta\varphi$, thus maintaining a zero phase shift around the feedback loop. The new oscillation frequency is given by

$$\omega = \omega_o + \Delta\omega = \omega_o \left[1 - \frac{1}{2} \sum_{n=2}^{\infty} d_n^2 (n^2 - 1) \right] \quad (5)$$

where ω_o is the nominal oscillation frequency without considering the nonlinear effects, and d_n represents the amplitude of the n th harmonic. It is obvious that if the band-pass system is selectively tuned to a central frequency ω_o and the overall loop-gain is close to unity, the output signal will be a pure sinusoid oscillating at the central frequency.

Low-pass filters can be cascaded with a simple high-pass RC filter to construct a BPF. Similarly, cascading a low-pass RC circuit with a high-pass filter results in a BPF. Existing low-pass and high-pass filters on the chip may be cascaded together to obtain a BPF. The input of a notch filter may be subtracted from its output to construct a BPF.

IV. ANALOG FAULT MODELING

In order to verify the fault coverage of the test method presented, an accurate and realistic fault list is required. A fault can be either parametric (soft) or catastrophic (hard). Parametric faults, caused by statistical fluctuations in the manufacturing process, comprise the small deviation of CUT parameters from their tolerance band. Catastrophic faults are introduced by random defects and result in failures in various components. They are provoked, for example, by dust particles on a photolithographic mask and cause either short and open circuits or large deviations of CUT parameters from their tolerance bands, such as the width-to-length (W/L) ratio of a MOS transistor [2], [16].

Many studies have been devoted to determining the dominant fault types and to defining appropriate fault models. Research results show that 80% to 90% of observed analog faults are catastrophic faults, consisting of shorts and opens in diodes, transistors, resistors and capacitances [17], [18]. These studies indicate that catastrophic faults, and especially short faults, are dominant in both bipolar and CMOS processing technologies.

In our case studies, the undetectable band of parametric faults is determined for all passive elements. The undetectable band of parametric faults for a passive component is defined as the variation region of the component maintaining the oscillation frequency within its tolerance band. A comprehensive list of catastrophic faults is also injected and simulated for all case studies. The catastrophic faults considered in this study comprise all open faults at all circuit nodes and short faults between every combination of two nodes at transistor level in opamps, and shorts for all other components. An open fault is simulated by introducing a 10 M Ω resistor. A short fault is modeled by a 10 Ω resistor.

V. CASE STUDIES AND RESULTS

Oscillation-test methodology has been applied to numerous types of low-pass, band-pass, high-pass, and notch filters. All case studies have been designed using CMOS 1.2 μm technology parameters of Nortel. A two-stage, CMOS operational amplifier has been employed to realize the active filters. All computer simulations have been performed in Analog Artist environment using HSPICE simulator. Simulation and practical results confirm that various oscillators with different oscillation frequencies and waveforms can be constructed from each type of filter. The choice of the oscillator may improve the fault coverage especially for parametric faults. It has been also found that each oscillator is more sensitive to a set of components and therefore by constructing more than one oscillator from the filter under test, the fault coverage may be improved. In the following sections, some case studies are briefly presented. The aim of this work is to show that oscillation-test strategy is able to detect the parametric faults as well as catastrophic faults. To quantify the fault coverage, a comprehensive list of catastrophic fault has been injected in operational amplifiers at transistor level. Generally, a fault coverage of better than 95% has been obtained for all case studies. Parametric and catastrophic faults have been also injected for all passive elements and the limit of detectable

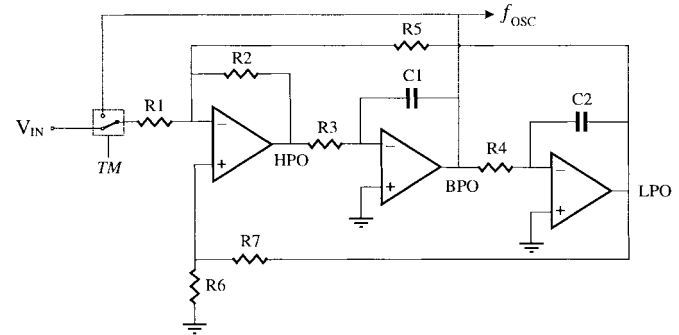


Fig. 2. Testable state-variable active filter. TM: Test-mode signal, HPO: high-pass output, BPO: band-pass output, LPO: low-pass output, $R_1 = R_2 = R_3 = R_4 = R_5 = 10 \text{ K}\Omega$, $R_6 = 1 \text{ K}\Omega$, $R_7 = 12 \text{ K}\Omega$, $C_1 = C_2 = 20 \text{ nF}$.

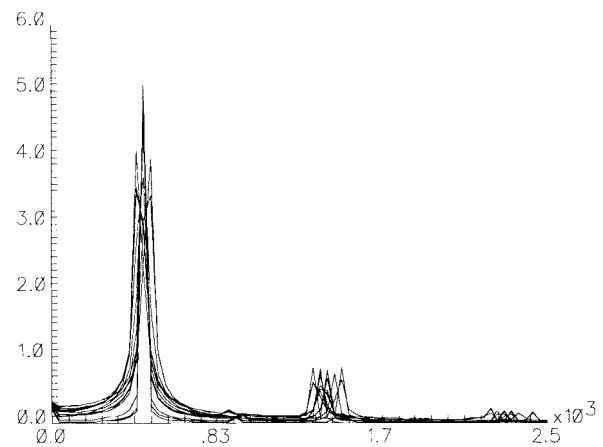


Fig. 3. Monte Carlo analysis of the BPF-based oscillator using a Gaussian distribution function and 15 iterations.

parametric faults has been specified. To verify the simulation results, all case studies have been also realized using μA 741 operational amplifiers and discrete components. The practical results confirm that both parametric and catastrophic faults are detectable.

A. Band-Pass Filter Testing

In this section, the problem of active band-pass filter testing is investigated. The circuit under test, shown in Fig. 2, is a state-variable filter which incorporates low-pass, high-pass and band-pass filters. For test purposes, its band-pass output is considered. The band-pass output has a central frequency of 750 Hz and a gain of 4.5. Band-pass filters (BPF's) can be converted to an oscillator using quite a simple technique. The basic principle consists in establishing a positive-feedback loop with a zero-crossing detector (ZCD) or a hard limiter. The wide-band noise at the input of the BPF is filtered and only a sine wave signal whose frequency is equal to the center frequency of the filter ω_o , where the lead and lag phase shifts cancel each other out, is passed. The ZCD produces a square wave at its output whose frequency is ω_o . This square wave is applied to the BPF input and the filter generates a sine wave at the fundamental frequency ω_o . The ZCD introduces a very high gain to guarantee sustained oscillation. It should

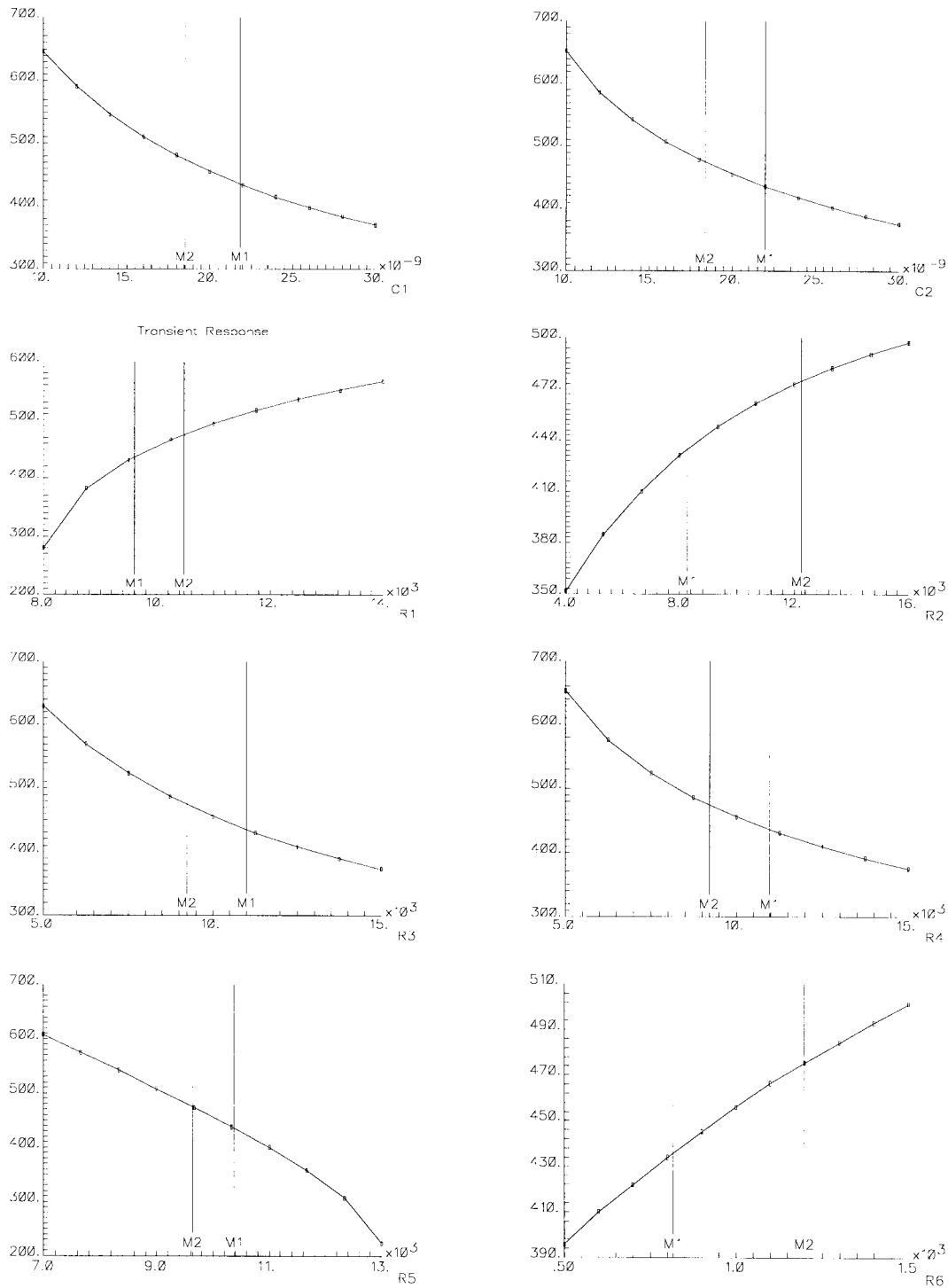


Fig. 4. The variations of the oscillation frequency of the BPF-based oscillator versus different passive components of the BPF.

be noted that if the filter gain at its passing band is greater than unity the ZCD is not necessary. The BPF under test in this example has a gain of approximately 4.5, and therefore the ZCD was not. During the test-mode, the TM signal is active which connects the BPO of the filter to its input to establish oscillations. Therefore, the area overhead is related to an analog switch. A loop-gain greater than unity causes saturation of the oscillating signal and therefore the oscillation signal contains many harmonics and its frequency deviates

from the central frequency of the filter, as explained using (5). The nominal oscillation frequency was approximately 455 Hz. In order to determine the tolerance band of the oscillation frequency, a Monte Carlo analysis with a Gaussian distribution function taking into account a 5% tolerance for all components has been performed. The fast Fourier transform (FFT) of the resulting output signal is illustrated in Fig. 3.

The lower and upper limits of the oscillation frequency tolerance band are approximately 441 Hz and 483 Hz (-3 and

6%), respectively. Fig. 4 illustrates the undetectable tolerance band, marked by M1 and M2, for each passive component which are also presented in Table I. The testable BPF was also realized using a μA 741 opamp and discrete resistor and capacitances. The results of practical realization are listed in Table II. Practical implementation and simulation results confirm that both catastrophic and parametric faults can be detected.

B. High-Pass Filter Testing

As mentioned before, a high-pass filter (HPF) can be cascaded with a simple low-pass RC circuit to form a BPF and then converted to an oscillator by connecting the output of the achieved BPF to its input. Because of the limited bandwidth of the operational amplifier employed, the active HPF is considered to be a band-pass system. Therefore an active HPF can be transformed to an oscillator by connecting its input and output together to establish a positive feedback as shown in Fig. 5. Thus, the area overhead consists of only an analog switch. The resulting fault-free oscillation frequency was approximately 6.284 KHz. Due to the large bandwidth of the filter, the oscillating signal contains significant harmonics. A Monte Carlo analysis with a Gaussian distribution function taking into account a 5% tolerance for all components determined a lower and upper limits of approximately 6.047 and 6.588 KHz (-3.8% and 4.8%), respectively. The undetectable tolerance band of parametric faults for each passive component are presented numerically in Table III. The testable HPF was realized in practice using a μA 741 opamp and discrete resistor and capacitances. The obtained results, presented in Table IV, show that both catastrophic and parametric faults are detectable. As the results indicate the oscillation frequency of the HPF-based oscillator employed is less sensible to R1 and R3. It should be noted that, the filter parameters are also less sensible to these components. Producing another oscillation frequency which is more sensible to these components may improve the parametric faults coverage. This kind of optimization is demonstrated for the last case study.

C. Low-Pass Filter Testing

The conventional method to convert an active low-pass filter (LPF) to an oscillator consists of establishing a positive feedback containing a simple high-pass RC circuit. The other approach is to relocate the filter poles onto the imaginary axis by modifying some passive components in the test-mode. The approach employed here, consists of adding a positive feedback comprising a high-gain inverter as shown in Fig. 6. The concept is similar to ring oscillators. The inverter guarantees 180° of phase shift and the LPF introduces a delay which controls the oscillation frequency. The inverter has been realized using minimum sized MOS transistors. The fault-free oscillation frequency was approximately 2.135 KHz. Monte Carlo analysis shows that the oscillating signal has a lower and upper limits of approximately 2.017 and 2.38 KHz (-5.5% and 11.4%). The undetectable tolerance band for each passive component of the LPF are numerically presented in Table V. The results indicate the limit of detectable parametric

TABLE I
UNDETECTABLE LIMITS OF THE PARAMETRIC
FAULTS IN PASSIVE COMPONENTS OF ACTIVE BPF

Component	Undetectable Limits	Component	Undetectable Limits
C1 (20 nF)	< -7.4% , 9% >	R4 (10 K Ω)	< -7.8% , 9.8% >
C2 (20 nF)	< -8.2% , 9.8% >	R5 (10 K Ω)	< -3.5% , 3.6% >
R1 (10 K Ω)	< -3.9% , 4.9% >	R6 (1 K Ω)	< -18% , 19% >
R2 (10 K Ω)	< -16.2% , 22% >	R7 (12 K Ω)	< -18.7% , 15% >
R3 (10 K Ω)	< -7.8% , 9.5% >		

faults for all passive components. The testable LPF was also realized using discrete components and the results confirm the simulation results.

D. Myoelectrical Signal Amplifier/Filter Testing

In this section, the oscillation-test method has been applied to test a practical filter circuit [20]. The idea of generating more than one oscillation frequency per building block and optimizing the set of oscillation frequencies is demonstrated through this example. The CUT is a simple amplifier and filter unit to interface myoelectrical signals from patient to computer [20]. Fig. 7 reveals the test solution for this circuit based on the method presented in this paper. During the normal operation of the circuit, S_1 selects V_{IN} , S_2 selects the ground, S_3 is closed, S_4 is open and S_5 is closed. Switches have been realized using a CMOS structure to minimize the undesired effects introduced due to their presence. Simulations using HSPICE, without and in the presence of switches confirm that there is no significant effect on the functionality of the CUT due to the existence of switches.

The technique employed in this section to convert the CUT to oscillators is to establish positive feedback for a band-pass system, which has a greater-than-unity gain in its pass-band. To increase the number of oscillation frequencies, the capacitor C , which is used to bypass the capacitor C_1 , has been added. As a result, six different oscillation frequencies can be produced using only two test points.

- 1) Switch S_1 selects the ground, S_2 selects the output of OA2, S_3 is closed, S_4 is open and S_5 is closed. The oscillation frequency f_{osc1} is observed at the output of OA2. All CUT components are involved in the test.
- 2) The same as in case 1, except that switch S_5 is open. The output of OA2, f_{osc2} , is used as the test point. All CUT components, except C_1 , are involved in the test.
- 3) Switch S_1 selects the ground, S_2 selects the positive input of OA2, S_3 is closed, S_4 is open and S_5 is closed. The oscillation frequency f_{osc3} is observed at the output of OA1. The components involved are R_1, R_2, R_3, C_1 , and OA1.
- 4) The same as in case 3, except that switch S_5 is open. The oscillation frequency f_{osc4} is observed at the output of OA1 to monitor the faults in R_1, R_2, R_3 , and OA1.
- 5) Switches S_1 and S_2 select the ground, S_3 is open, S_4 is closed and S_5 is closed. The oscillation frequency f_{osc5} is observed at the output of OA2. The components involved are R_3, R_4, R_5, C_1, C_2 , and OA2.

TABLE II
PRACTICAL RESULTS OF THE INJECTED PARAMETRIC AND CATASTROPHIC FAULTS IN THE STATE-VARIABLE ACTIVE FILTER CIRCUIT

Component	C1	C2	R1	R2	R3	R4	R5	R6	R7
$\Delta C/C$	Short	Short	Short	Short	Short	Short	Short	Short	Short
$\Delta f_{osc}/f_{osc}$	NO	NO	NO	NO	+215%	+1830%	+109%	NO	NO
$\Delta C/C$	Open	Open	Open	Open	Open	Open	Open	Open	Open
$\Delta f_{osc}/f_{osc}$	+219%	+1980%	NO	+41%	NO	NO	NO	NO	NO
$\Delta C/C$	-25%	-25%	-30%	-20%	-20%	-20%	-20%	-20%	+17%
$\Delta f_{osc}/f_{osc}$	+21%	18%	-20%	-7.5%	+17%	+12.5%	+34%	-6%	-11%
$\Delta C/C$	-50%	-50%	-55%	-50%	-50%	-50%	-50%	-50%	+65%
$\Delta f_{osc}/f_{osc}$	+57%	31%	-51%	-18%	+46%	+42%	+62%	-31%	-30%
$\Delta C/C$	+25%	+25%	+20%	+50%	+20%	+20%	+15%	+20%	+100%
$\Delta f_{osc}/f_{osc}$	-11%	-12%	+19%	+10	-11%	-12%	-29%	+9%	-51%
$\Delta C/C$	+50%	+50%	+50%	+100%	+50%	+50%		+50%	
$\Delta f_{osc}/f_{osc}$	-20%	-19%	+39%	+19	-22%	-22%		+12%	

$\Delta C/C$: Percentage of the faults injected into component C , $\Delta f_{osc}/f_{osc}$: Variation of the oscillation frequency from its nominal value, NO: No oscillation.

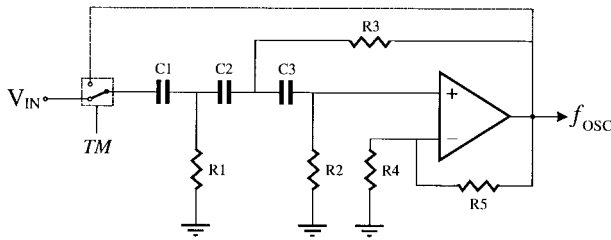


Fig. 5. Testable active high-pass filter TM: Test-mode signal, $R_1 = 1$ K Ω , $R_2 = R_3 = 10$ K Ω , $R_4 = R_5 = 39.2$ K Ω , $C_1 = C_2 = C_3 = 16$ nF.

TABLE III
UNDETECTABLE LIMITS OF THE PARAMETRIC
FAULTS IN PASSIVE COMPONENTS OF ACTIVE HPF

Component	Undetectable Limits	Component	Undetectable Limits
C1 (160 nF)	< -19% , 3.2% >	R2 (10 K Ω)	< -8.9% , 1.5% >
C2 (16 nF)	< -19.5% , 2.5% >	R3 (10 K Ω)	< -32% , 150% >
C3 (16 nF)	< -15.6% , 2.8% >	R4 (39.2 K Ω)	< -1.8% , 9.5% >
R1 (1 K Ω)	< -68% , 380% >	R5 (39.2 K Ω)	< -8.6% , 2% >

TABLE IV
PRACTICAL RESULTS OF THE INJECTED PARAMETRIC AND
CATASTROPHIC FAULTS IN THE HIGH-PASS FILTER CIRCUIT

Component	C1	C2	C3	R1	R2	R3	R4	R5
$\Delta C/C$	-20%	-20%	-20%	-70%	-20%	-20%	-20%	-20%
$\Delta f_{osc}/f_{osc}$	+5%	+4.8%	+9%	+6%	+13%	-3%	-17%	+16%
$\Delta C/C$	-50%	-50%	-50%	+400%	-50%	-50%	-50%	-50%
$\Delta f_{osc}/f_{osc}$	+21%	+23%	+26%	-5.5%	+30%	-14%	-36%	+49%
$\Delta C/C$	+20%	+20%	+20%	+1000%	+20%	+100%	+20%	+20%
$\Delta f_{osc}/f_{osc}$	-12%	-10%	-11%	-9%	-15	+4%	+9.5%	-13%
$\Delta C/C$	+50%	+50%	+50%		+50%	+200%	+50%	+50%
$\Delta f_{osc}/f_{osc}$	-17%	-16%	-19%		-26	+6.5%	+28%	-23%

$\Delta C/C$: Percentage of the faults injected into component C , $\Delta f_{osc}/f_{osc}$: Variation of the oscillation frequency from its nominal value, NO: No oscillation.

- 6) The same as in case 5, except that switch S_5 is open. The oscillation frequency f_{osc6} is observed at the output of OA2 to detect the faults in R_1, R_2, R_3 , and OA1.

The testable amplifier/filter, shown in Fig. 7, has been realized using μA 741 and discrete elements. Available CMOS analog switches, DGP201A from Siliconix Inc., have been used to convert the CUT to oscillators. All possible shorts

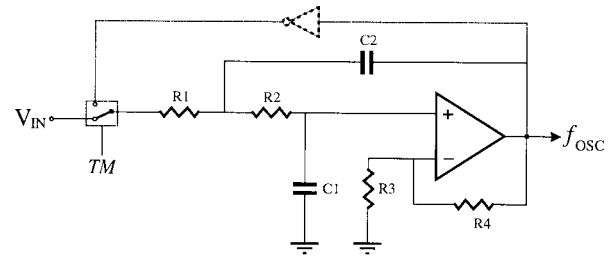


Fig. 6. Testable active low-pass filter. TM: Test-mode signal, $R_1 = R_2 = 3.2$ K Ω , $R_3 = 4.86$ K Ω , $R_4 = 8.84$ K Ω , $C_1 = C_2 = 50$ nF. The switch position shows the filter in its normal mode.

TABLE V
UNDETECTABLE LIMITS OF THE PARAMETRIC
FAULTS IN PASSIVE COMPONENTS OF ACTIVE LPF

Component	Undetectable Limits	Component	Undetectable Limits
R1 (3.2 K Ω)	< -15% , 5.3% >	R4 (8.84 K Ω)	< -9.3% , 2.7% >
R2 (3.2 K Ω)	< -54% , 125% >	C2 (50 nF)	< -6% , 2% >
R3 (4.86 K Ω)	< -14% , 10% >	C1 (50 nF)	< -4% , 13% > & < -50% , -68% >

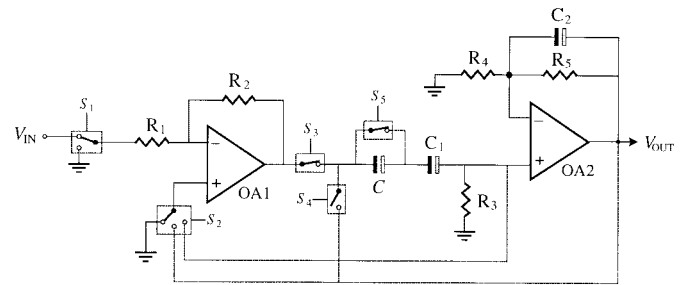


Fig. 7. Practical myoelectrical signal amplification and filtering circuit and its test solution based on oscillation-test method. $R_1 = 10$ K Ω , $R_2 = 330$ K Ω , $R_3 = 1$ M Ω , $R_4 = 10$ K Ω , $R_5 = 330$ K Ω , $C_1 = 330$ nF, $C_2 = 4.7$ nF, and $C = 50$ pF.

and opens on resistors and capacitors have been injected. Furthermore, 20% and 50% of deviations from the nominal value in both directions have been introduced for all passive components. All catastrophic faults, except open at C_2 , are detectable using only the first oscillator which produces f_{osc1} . The fault at C_2 is detected using the second oscillation frequency f_{osc2} .

TABLE VI
PRACTICAL RESULTS OF INJECTING PARAMETRIC FAULTS INTO THE MYOELECTRICAL
AMPLIFIER/FILTER CIRCUIT. CATASTROPHIC FAULTS ARE NOT PRESENTED IN THIS TABLE

Fault	Δf_{osc1}	Δf_{osc2}	Δf_{osc3}	Δf_{osc4}	Δf_{osc5}	Δf_{osc6}	Fault	Δf_{osc1}	Δf_{osc2}	Δf_{osc3}	Δf_{osc4}	Δf_{osc5}	Δf_{osc6}
	f_{osc1}	f_{osc2}	f_{osc3}	f_{osc4}	f_{osc5}	f_{osc6}		f_{osc1}	f_{osc2}	f_{osc3}	f_{osc4}	f_{osc5}	f_{osc6}
$R_1(20\% \downarrow)$	-4%	-5.5%	-6.5%	-7.8%	NI	NI	$R_4(50\% \downarrow)$	-7.8%	-3.5%	NI	NI	-14%	-41%
$R_1(20\% \uparrow)$	3.9%	7%	6.2%	7%	NI	NI	$R_4(50\% \uparrow)$	6.5%	4%	NI	NI	12%	NO
$R_1(50\% \downarrow)$	-8%	-13%	-13%	-14%	NI	NI	$R_5(20\% \downarrow)$	4.9%	29%	NI	NI	8%	10.7%
$R_1(50\% \uparrow)$	5.5%	14.5%	11.5%	12%	NI	NI	$R_5(20\% \uparrow)$	-3.5%	-19%	NI	NI	-6%	-23%
$R_2(20\% \downarrow)$	3.9%	9.5%	7.4%	7.5%	NI	NI	$R_5(50\% \downarrow)$	9.9%	97%	NI	NI	20%	31%
$R_2(20\% \uparrow)$	-4.5%	-5%	-6%	-6%	NI	NI	$R_5(50\% \uparrow)$	-5.5%	-35%	NI	NI	-9.8%	-22%
$R_2(50\% \downarrow)$	8.3%	24.8%	20%	19.9%	NI	NI	$C_1(20\% \downarrow)$	29.5%	NI	29.3%	NI	29%	NI
$R_2(50\% \uparrow)$	-7%	-13%	-11%	-12%	NI	NI	$C_1(20\% \uparrow)$	-19%	NI	-19%	NI	-19%	NI
$R_3(20\% \downarrow)$	27%	8.5%	27.3%	27%	27.3%	NO	$C_1(50\% \downarrow)$	101%	NI	100%	NI	100%	NI
$R_3(20\% \uparrow)$	-19%	-4%	-19%	-20%	-19%	-40%	$C_1(50\% \uparrow)$	-35%	NI	-35%	NI	-35%	NI
$R_3(50\% \downarrow)$	103%	15.5%	103%	103%	102%	NO	$C_2(20\% \downarrow)$	1.2%	27.6%	NI	NI	0.8%	-31%
$R_3(50\% \uparrow)$	-35%	-5.6%	-35%	-35%	-35%	-55%	$C_2(20\% \uparrow)$	-1.5%	-19%	NI	NI	-1%	NO
$R_4(20\% \downarrow)$	-3.8%	-2.5%	NI	NI	-6.5%	-35%	$C_2(50\% \downarrow)$	1.6%	94.5%	NI	NI	1.1%	-31%
$R_4(20\% \uparrow)$	4.2%	1.5%	NI	NI	6.2%	NO	$C_2(50\% \uparrow)$	-2%	-35%	NI	NI	-1.5%	NO

NO: No oscillation, NI: Not involved in the test.

Table VI presents the effects of injected parametric faults on the oscillation frequencies produced. The sensitivity of different oscillation frequencies with respect to a given injected fault changes, depending on the relationship between the faulty component and the oscillation frequencies. To reduce the complexity of the test procedure keeping high fault coverage, redundant or nonefficient tests must be removed by identifying the most sensitive oscillation frequency for each injected fault. The most effective oscillation frequency is marked in Table VI for each fault. It is noteworthy that in the majority of cases the output frequencies, f_{osc3} , f_{osc4} , and f_{osc5} are less sensitive than f_{osc1} , f_{osc2} , and f_{osc6} . In other words, f_{osc3} , f_{osc4} , and f_{osc5} do not cover any fault that cannot be covered by f_{osc1} , f_{osc2} , and f_{osc6} . Therefore, the oscillation frequencies, f_{osc3} , f_{osc4} , and f_{osc5} can be eliminated to minimize the test procedure. As all remaining oscillation frequencies are observed at the output of OA2, the test point taken out from the output of OA1 is eliminated and therefore only one test point is sufficient to monitor 100% of injected catastrophic and parametric faults in this example.

VI. PRACTICAL CONSIDERATIONS AND DISCUSSION

In this section some practical considerations and guidelines for successful and efficient implementation of the proposed test techniques are discussed.

A. Analog Switches

Switches are the key components in analog testing and provide the programmability of the test structure. The accuracy of the switches directly affects the accuracy, and therefore the functionality, of the test system, especially when we deal with low-voltage signals and where high measurement precision is sought. Due to its nonideal characteristics, it may cause serious performance degradation of the circuit under test. The most important characteristics of a switch are its "on" resistance R_{ON} , its "off" resistance R_{OFF} , and the values of its parasitic capacitors.

The R_{ON} and R_{OFF} values affect the transparency of the switches in the test structure. For switches to be transparent in the CUT and not degrade its performance, their R_{ON} must be as low as possible and their R_{OFF} must be as high as possible. Parasitic capacitors determine the clock feedthrough and charge injection error values introduced by the switch. To minimize the clock feedthrough error, the parasitic capacitors must be as low as possible. Using a CMOS switch or a dummy transistor and a symmetrical switching procedure, feedthrough error can be diminished through cancellation [19]. Careless design of test switches may cause instability problems in critical designs due to the presence of parasitic capacitances.

The R_{ON} of a MOS switch and its thermal noise contribution can be reduced by increasing the W/L ratio. The $1/f$ noise contribution of MOS switches can be reduced by increasing their W and L . Increasing W and L arbitrarily increases the parasitic capacitor values and consequently increases the feedthrough effect. A compromise must therefore be made to satisfy all requirements.

In the test structures presented in this paper, the switches can be divided into two main categories depending on their application:

- 1) switches appearing in the signal path of the CUT, such as switches which divide the CUT into building blocks;
- 2) switches which are not inserted in the signal path, like switches used to establish feedback loops.

The first category of switches must be realized using CMOS switches to minimize R_{ON} . Reducing R_{ON} decreases the degradation of the signal amplitude and reduces the instability problems. As no precision voltage measurement is required in this test method and clock feedthrough has no effect on the test performance, the second category of switches can be realized simply using a minimum-sized NMOS transistor.

B. Fault Coverage

There are three sources of imprecision in analog testing: the imprecision related to the analog test stimulus applied, the acceptable tolerance of the CUT and the imprecision

of output checkers. During the test process, the acceptable performance deviation range must be enlarged to accommodate these sources of error because they may exist even if the CUT is fault-free. In the proposed test technique, the first source of error is eliminated because no test vector is applied. The third error source is also minimized, because the parameter to be measured is a frequency rather than a voltage which is easily converted to a number without significant precision degradation. Furthermore the oscillation frequency is less sensible to noise.

In a given oscillator, the oscillation frequency depends on a wide range in the ac behavior of its transfer function with variable sensitivities. For example, in the band-pass based oscillator described in this paper, the oscillation frequency depends on the entire range of its open-loop ac behavior having a gain greater than unity. In fact, the oscillation frequency can be considered as the sum of frequency components which can pass through the band-pass system with amplification. Therefore, a change in any of these components will affect the oscillation frequency. When testing this band-pass system with a specified test frequency, based on conventional test methods, reliable information about the ac behavior of the rest of the transfer function cannot be achieved. In practice, many test frequencies should be applied to ensure complete coverage over the ac behavior of the CUT. The sum of these test frequencies can be applied to the band-pass system as a multitone test frequency. In this case, the ac behavior coverage is comparable to the coverage obtained by evaluating the oscillation frequency in the oscillation-test strategy.

Finally, as stated previously, by producing different oscillation frequencies from the CUT and optimizing the number of oscillation frequencies versus the fault coverage.

C. Design-for-Test Procedure Automation

The simplicity of DFT techniques presented is very promising for automatic generation of testable filters. Therefore the DFT techniques discussed above, can be integrated in filter synthesis tools. Given the design of a conventional active filter and having developed efficient and simple techniques to transform a filter to an oscillator, the following steps must be pursued.

- 1) The filter under test is converted to main possible oscillators and the nominal oscillation frequencies are determined.
- 2) A Monte Carlo analysis is performed for all oscillators to determine the tolerable variations of the output oscillation frequency for each oscillator.
- 3) Based on the tolerance band of the oscillation frequency of each oscillator obtained from step 2, the undetectable band of parametric fault is determined for all passive elements for each oscillator.
- 4) The catastrophic fault coverage of operational amplifiers is also evaluated for all oscillators.
- 5) Based on the predetermined fault coverage specified by the designer and results obtained from steps 3 and 4, a minimal number of oscillators are determined to obtain the required fault coverage.

- 6) Stability analysis of achieved testable filter is performed and overhead reduction of MOS switches is effectuated.
- 7) The number of control lines and the control logic is optimized based on remaining oscillators.

VII. CONCLUSIONS

In this paper, we have introduced novel DFT techniques for active analog filters based on a new vectorless digital-output test methodology. As an on-chip stimulus generator is not required and the test output is a digital signal, the DFT techniques can be implemented with very little, and simple, hardware overhead. In the majority of cases, the area overhead is composed of only some analog switches. The robustness of the test scheme presented has been demonstrated through extensive simulations and practical implementations of various active analog filter. As only oscillation frequency is evaluated to detect faults, the introduced DFT techniques are immune to noise. Finally, the DFT techniques investigated are very suitable for automatic testable filter synthesis and can be easily integrated in the tools dedicated to automatic filter design.

ACKNOWLEDGMENT

The authors would like to acknowledge the efforts of B. Shaiek in obtaining the results of practical implementations.

REFERENCES

- [1] K. Arabi, B. Kaminska, and J. Rzeszut, "BIST for digital-to-analog and analog-to-digital converters," *IEEE Design Test Comput.*, vol. 13, no. 4, pp. 40–49, 1996.
- [2] M. J. Ohletz, "Hybrid built-in self-test (HBIST) structure for mixed analog/digital integrated circuits," *2nd Eur. Test Conf.*, 1991, pp. 307–316.
- [3] A. Chatterjee, K. Bruce, and N. Nagi, "DC built-in self-test of linear analog circuits using checksums," in *VLSI Design Symp.*, Bangalore, India, 1996.
- [4] M. Soma, "A design-for-test methodology for active analog filters," in *IEEE Int. Test Conf.*, 1990, pp. 183–192.
- [5] J. L. Huertas, A. Rueda, and D. Vazquez, "Testable switched-capacitor filters," *IEEE J. Solid-State Circuits*, vol. 28, no. 7, 1993.
- [6] M. Jarwala and S.-J. Tsai, "A framework for design for testability of mixed analog/digital circuits," in *IEEE Custom Integrated Circuit Conf.*, 1991, pp. 13.5.1–13.5.4.
- [7] P. P. Fasang, D. Mulins, and T. Wong, "Design for testability for mixed analog/digital ASICs," *IEEE Custom Integrated Circuit Conf.*, 1988, pp. 16.5.1–16.5.4.
- [8] K. D. Wagner and T. W. Williams, "Design for testability of mixed signal integrated circuits," *IEEE Int. Test Conf.*, 1988, pp. 823–829.
- [9] C.-L. Wey, "Built-in self-test structure for analog circuit fault diagnosis," *IEEE Trans. Instrum. Meas.*, vol. 39, no. 3, pp. 517–521, 1990.
- [10] L. T. Wurtz, "Built-in self-test structure for mixed-mode circuits," *IEEE Trans. Instrum. Meas.*, vol. 42, pp. 25–29, Feb. 1993.
- [11] K. Arabi and B. Kaminska, "Testing analog and mixed-signal integrated circuits using oscillation-test method," *IEEE Trans. Computer-Aided Design*, vol. 16, pp. 745–753, July 1997.
- [12] ———, "Design for testability of embedded integrated operational amplifiers," *IEEE J. Solid-State Circuits*, vol. 33, pp. 573–581, Apr. 1998.
- [13] K. Arabi *et al.*, "Dynamic digital integrated circuit testing using oscillation-test method," *Electron. Lett.*, vol. 34, no. 8, pp. 762–763, 1998.
- [14] D. Vazquez, A. Rueda, and J. L. Huertas, "A low-cost strategy for testing analog filters," in *IEEE Int. Symp. Circuits Systems*, 1994, pp. 123–126.
- [15] K. K. Clarke and D. T. Hess, *Communication Circuits: Analysis and Design*. Reading, MA: Addison-Wesley, 1971, p. 658.
- [16] L. Milor and V. Visvanathan, "Detection of catastrophic faults in analog integrated circuits," *IEEE Trans. Computer-Aided Design*, vol. 8, pp. 114–130, Feb. 1989.
- [17] C. Stapper, F. Armstrong, and K. Saji, "Integrated circuit yield statistics," *Proc. IEEE*, vol. 71, pp. 453–470, 1983.

- [18] Q. F. Wilson and D. B. Day, "Practical automatic test program generation constraints," in *Proc. Automatic Test Conf. Workshop*, 1987.
- [19] P. Allen and D. R. Holberg, *CMOS Analog Circuit Design*. New York: Holt, Rinehart, and Winston, 1987.
- [20] F. Aubain, M. Slamani, and B. Kaminska, "BIOLINK: A new myoelectrical pointing device for interactive computer systems," *IEEE EMBS Conf.*, 1991, pp. 1847-1848.

Karim Arabi (M'94) received the B.Sc. degree in electronics engineering from Tehran Polytechnic, Tehran, Iran, in 1989, and the M.Sc. and Ph.D. degrees in electrical engineering from the École Polytechnique, Montreal, P.Q., Canada, in 1993 and 1996 respectively.

He is a founder of Opmaxx, Inc., Beaverton, OR, where he was responsible for built-in self-test product development from 1996 to 1998. He is currently a Professor at the École de Technologie Supérieure (ÉTS), Montreal. His main research interests include various aspects of design, test and reliability of high-performance analog and mixed-signal integrated circuits. He has published more than 50 technical papers in the above mentioned fields.

Dr. Arabi is a founding member of International Functional Electrical Stimulation Society (IFESS) and a Program Committee Member of the IEEE International Conference on Computer Design.

Bozena Kaminska (M'88-SM'99) received the Ph.D. degree in microelectronics from Warsaw Technical University, Warsaw, Poland.

She has extensive background in CAE/CAD, system design, and IC design and is Senior Vice President and Chief Technical Officer of Opmaxx Inc., Beaverton, OR. For the past 13 years, she has been affiliated with Ecole Polytechnique de Montreal, Montreal, P.Q., Canada. Her main research interests include analog and mixed-signal design automation and test of analog systems. She is the author or co-author of more than 100 papers in these areas and holds several patents.

Dr. Kaminska is chair of the IEEE Test Technology Technical Committee on Mixed-Signal Testing. She is a program committee member of various organizations including the IEEE VLSI Test Symposium, International Test Conference, Asian Test Symposium, IEEE Workshops on mixed-signal testing, on-line testing, and defect and fault tolerance.